CHAPTER-3

An investigation on coupled thermoelastic interactions in a thick plate due to axi-symmetric temperature distribution under an exact heat conduction with a delay

3.1 Introduction

Recently, Quintanilla and Racke (2006) have explained the stability of the approximated two phase-lag heat conduction model given by Tzou (1995*a,b*). In the frame of dual phase-lag thermoelastic model, an alternative extension of GN-III model is introduced by Roychoudhuri (2007*a*) which is called as three phase-lag model. With a detailed discussion regarding the stability of this model as well as the mathematical consistency of three phase-lag and dual-lag model, Quintanilla (2011) has recently proposed to re-formulate the three phase-lag heat conduction model and suggested an alternative heat conduction theory with a single delay term. Quintanilla (2011) has further considered the Taylor series approximation in the thermal gradient part of the proposed constitutive law. In the previous chapter, the comparative study of four different thermoelastic models with respect to a thick plate problem has been carried out. The main purpose of this chapter is to examine the effects of the single phase-lag parameter/delay term on wave propagation inside a thick plate due to the thermoelastic interactions caused by thermo-mechanical loading applied at the boundary surface of the plate. In order to investigate the effects of the single delay time parameter, we have considered two versions of the new model by taking the first three and two terms of Taylor series approximation. We call them as new model-I (Quintanilla-I) and new model-II (Quintanilla-II) for our study.

This work is published in ***International Journal of Thermal Sciences (Elsevier)***, 159-173, 110 (2016).

We consider a coupled dynamical thermoelastic problem of an infinitely extended thick plate and present a complete analysis of the effects of single delay term on the wave propagation inside the medium. The lower and upper surfaces of the plate are considered to be stress free and are subjected to a given axi-symmetric temperature distribution. The nature of distributions of different fields inside the thick plate under this temperature distribution are investigated. We firstly write the unified basic governing equations in the contexts of four models, namely new model-I, new model-II, model of type GN-III and Lord-Shulman (LS) model. The problem under LS-model which also includes one thermal relaxation time parameter was investigated by Sherief and Hamza (1994). We make an attempt to compare the results in the present context with the results under LS-model reported in Sherief and Hamza (1994) and present a complete analysis on the wave propagation and nature of discontinuities of different fields under different models as mentioned above. In the last section, we present numerical solution of the problem and illustrate the behavior of different fields like, temperature, displacement and stresses in the middle plane of the plate. Results are displayed graphically. Analysis of the results obtained under new models along with a comparison of the respective results obtained in other models including LS-model is presented. We observe a significant difference in the analytical as well as numerical results predicted by the present new models and the LS-model. However, we note some similarities in the results predicted by the present model and GN-III model. Therefore, the findings in the present work are believed to bring out some lights concerning the new heat conduction model that involves a single delay parameter.

3.2 Governing equations

The **equations** involving the stress, displacement and thermal fields in the absence of external body forces in a homogeneous and isotropic medium can be written as

$$\sigma_{ij,j} = \rho \ddot{u}_i \tag{3.1}$$

$$\sigma_{ij} = \lambda\, e\, \delta_{ij} + 2\mu e_{ij} - \gamma(T - T_0)\delta_{ij} \tag{3.2}$$

$$e_{ij} = \frac{1}{2}(u_{i,j} + u_{j,i}) \tag{3.3}$$

The heat conduction equation in the absence of heat source under **GN-III model** can be written as

$$[K^* + K\frac{\partial}{\partial t}]\nabla^2 T = (\rho\, c_e \ddot{T} + \gamma T_0 \ddot{e}) \tag{3.4}$$

We consider the corresponding heat conduction equation in the context of **new model-I** (see Quintanilla (2011)) as

$$[K^*(1 + \tau\frac{\partial}{\partial t} + \frac{\tau^2}{2}\frac{\partial^2}{\partial t^2}) + K\frac{\partial}{\partial t}]\nabla^2 T = (\rho\, c_e \ddot{T} + \gamma T_0 \ddot{e}) \tag{3.5}$$

The corresponding heat conduction equation in the context of **new model-II** (see Quintanilla (2011)) is given by

$$[K^*(1 + \tau\frac{\partial}{\partial t}) + K\frac{\partial}{\partial t}]\nabla^2 T = (\rho\, c_e \ddot{T} + \gamma T_0 \ddot{e}) \tag{3.6}$$

The heat conduction equation in the context of **LS-model** is given by

$$K\nabla^2 T = (1 + \tau_0\frac{\partial}{\partial t})(\rho\, c_e \dot{T} + \gamma T_0 \dot{e}) \tag{3.7}$$

In above equations, T and T_0 are the absolute temperature and reference temperature, respectively. τ_0 is a constant with the dimension of time that acts as the thermal relaxation time parameter under LS-model, while τ is the delay time as described by Quintanilla (2011). K and K^* are the thermal conductivity and the rate of thermal conductivity, respectively. u_i's are the components of the displacement field. $\gamma = (3\lambda + 2\mu)\alpha_t$, where α_t is the coefficient of linear thermal expansion parameter and e is the dilatation which is expressed as

$$e = e_{ii} \tag{3.8}$$

After combining the heat conduction equations given by Eqs. (3.4-3.7), the resultant equation can be rewritten in a unified way under above four models as

$$\left[[\delta_{1k}\left\{K^*(1+\tau\frac{\partial}{\partial t}+\tau_1\frac{\partial^2}{\partial t^2})+K\frac{\partial}{\partial t}\right\}+K\delta_{2k}]\right]\nabla^2 T = \left[\delta_{1k}\frac{\partial}{\partial t}+\delta_{2k}(1+\tau_0\frac{\partial}{\partial t})\right]\left[\rho\, c_e\dot{T}+\gamma T_0\dot{e}\right] \tag{3.9}$$

where, $\tau_1=\frac{\tau^2}{2}$

Then, we can find individual heat conduction equation under different models by putting different values of the delay time and values of k in the Kronecker delta δ_{ik} $(i=1,2)$ as given below:

- **GN-III model:** $k=1,\ \tau=0,\ K^*>0$
- **New model-I:** $k=1,\ \tau\neq 0,\ \tau_1\neq 0,\ K^*>0$
- **New model-II:** $k=1,\ \tau\neq 0,\ \tau_1=0,\ K^*>0$
- **LS model:** $k=2,\ \tau_0\neq 0$

Therefore, GN-III model, new model-I, new model-II and LS model can be studied simultaneously by considering the field equations given by (3.1-3.3) and Eq. (3.9) for u_i and T.

3.3 Formulation of the problem

Let us consider a problem of homogeneous, isotropic and infinitely extended thick plate of thickness $2l$ which is in an undisturbed state and initially at uniform temperature T_0. The z-axis is taken to be the axis of symmetry and the middle point between the lower and upper surfaces of the plate is taken to be the origin of the cylindrical polar coordinates (r,θ,z). Then for the medium in the region R defined by

$$R=\{(r,\theta,z):\ 0\leq r\leq\infty, 0\leq\theta\leq 2\pi, -l\leq z\leq l\}$$

The displacement components in the r and z directions are denoted by $u = u(r, z, t)$ and $w = w(r, z, t)$, respectively.

Therefore, Eq. (3.1) can be written as

$$\frac{\partial \sigma_{rr}}{\partial r} + \frac{\partial \sigma_{rz}}{\partial z} + \frac{\sigma_{rr} - \sigma_{\theta\theta}}{r} = \rho \frac{\partial^2 u}{\partial t^2} \tag{3.10}$$

$$\frac{\partial \sigma_{rz}}{\partial r} + \frac{\partial \sigma_{zz}}{\partial z} + \frac{\sigma_{rz}}{r} = \rho \frac{\partial^2 w}{\partial t^2} \tag{3.11}$$

We introduce the following non-dimensional quantities:

$c_1^2 = \frac{\lambda+2\mu}{\rho},\ r' = c_1\eta\, r,\ u' = c_1\eta\, u,\ t' = c_1^2\eta t,\ \tau_1' = c_1^4\eta^2\tau_1,\ \tau_0' = c_1^2\eta\,\tau_0,\ a_2 = \frac{\gamma}{K\eta},\ a_0 = \frac{K^*}{Kc_1^2\eta},$
$\xi = c_1\eta\, a,\ \lambda_1 = \frac{\lambda}{\mu},\ \beta = \frac{a_1}{\mu_1},\ \tau' = c_1^2\eta\,\tau,\ T' = \frac{T-T_0}{T},\ \sigma_{rr}' = \frac{\sigma_{rr}}{\mu},\ \sigma_{\theta\theta}' = \frac{\sigma_{\theta\theta}}{\mu},\ \mu_1 = \frac{\mu}{\lambda+2\mu},\ a_1 = \frac{\gamma T_0}{(\lambda+2\mu)}$

For the convenience, we drop the prime notations from all the quantities. Therefore, the dimensionless stress components derived from Eq. (3.2) are given by

$$\sigma_{rr} = 2\,e_{rr} + \lambda_1 e - \beta\, T \tag{3.12}$$

$$\sigma_{\theta\theta} = 2\,e_{\theta\theta} + \lambda_1 e - \beta\, T \tag{3.13}$$

$$\sigma_{zz} = 2\,e_{zz} + \lambda_1 e - \beta\, T \tag{3.14}$$

$$\sigma_{rz} = 2\,e_{rz} \tag{3.15}$$

where, non-dimensional strain components can be written as

$$e_{rr} = \frac{\partial u}{\partial r},\ e_{\theta\theta} = \frac{u}{r},\ e_{zz} = \frac{\partial w}{\partial z},\ e_{rz} = \frac{1}{2}\left(\frac{\partial u}{\partial z} + \frac{\partial w}{\partial r}\right)$$

Equations (3.9-3.11) can be written in the following non dimensional forms:

$$\left[\delta_{1k}\left\{a_0(1+\tau\frac{\partial}{\partial t}+\tau_1\frac{\partial^2}{\partial t^2})+\frac{\partial}{\partial t}\right\}+\delta_{2k}\right]\nabla^2 T = \left[\delta_{1k}\frac{\partial}{\partial t}+\delta_{2k}(1+\tau_0\frac{\partial}{\partial t})\right]\left[\dot{T}+a_2\dot{e}\right] \tag{3.16}$$

$$\mu_1\nabla^2 u-\mu_1\frac{u}{r^2}+(1-\mu_1)\frac{\partial e}{\partial r}-a_1\frac{\partial T}{\partial r}=\frac{\partial^2 u}{\partial t^2} \tag{3.17}$$

$$\mu_1\nabla^2 w+(1-\mu_1)\frac{\partial e}{\partial z}-a_1\frac{\partial T}{\partial z}=\frac{\partial^2 w}{\partial t^2} \tag{3.18}$$

where,

$$\nabla^2=(\frac{\partial^2}{\partial r^2}+\frac{1}{r}\frac{\partial}{\partial r}+\frac{\partial^2}{\partial z^2})$$

We use Helmholtz decomposition to find the displacement components u and w in the forms:

$$u=\frac{\partial\phi}{\partial r}+\frac{\partial^2\psi}{\partial r\partial z} \tag{3.19}$$

$$w=\frac{\partial\phi}{\partial z}-\frac{\partial^2\psi}{\partial r^2}-\frac{1}{r}\frac{\partial\psi}{\partial r} \tag{3.20}$$

Here, the potential functions ϕ and ψ are representing the dilatation and rotational part of displacement vector. We also find

$$e=\nabla^2\phi \tag{3.21}$$

In view of Eqs. (3.19-3.21) and (3.16-3.18), we constitute a system of equations involving the displacement potentials ϕ and ψ and the temperature field T as

$$\{[\delta_{1k}\{a_0(1+\tau\frac{\partial}{\partial t}+\tau_1\frac{\partial^2}{\partial t^2})+\frac{\partial}{\partial t}\}+\delta_{2k}]\nabla^2-[\delta_{1k}\frac{\partial}{\partial t}+\delta_{2k}(1+\tau_0\frac{\partial}{\partial t})]\frac{\partial}{\partial t}\}T$$
$$=a_2[\delta_{1k}\frac{\partial}{\partial t}+\delta_{2k}(1+\tau_0\frac{\partial}{\partial t})]\frac{\partial}{\partial t}\nabla^2\phi \tag{3.22}$$

$$\nabla^2\phi-\frac{\partial^2\phi}{\partial t^2}=a_1T \tag{3.23}$$

$$\nabla^2\psi-\frac{1}{\mu_1}\frac{\partial^2\psi}{\partial t^2}=0 \tag{3.24}$$

Eqs. (3.22-3.24) clearly indicate that ϕ and T are coupled together while ψ does not depend on ϕ and T. This implies that Eq. (3.24) represents the shear motion which is not affected by the thermal field and it is purely elastic in nature. However, Eqs. (3.22-3.23) represent the field functions ϕ and T included in the coupled thermoelastic motion.

3.4 Boundary conditions

Our assumptions regarding the present problem formulation show that both the upper and lower planes of the plate are traction free which implies that the mechanical boundary conditions are taken to be as

$$\sigma_{zz}(r,\pm l,t)=0,\ \ \sigma_{rz}(r,\pm l,t)=0 \tag{3.25}$$

We assume that the temperatures of the lower and upper surfaces of the plate suddenly increases at time $t=0$ such that the temperature of a circular region $r\leq a$ of both the upper and lower boundaries receive a fixed value C_0. That is, we assume

$$T(r,\pm l,t)=C_0H(a-r)H(t) \tag{3.26}$$

where, $H(t)$ is the Heaviside unit step function.

3.5 Solution of the problem

3.5.1 Laplace and Hankel transforms

In a similar way like the previous chapter, we firstly apply Laplace and Hankel transform technique to obtain the solution of the problem.

Therefore, assuming homogeneous initial conditions and applying the Laplace and Hankel transforms to Eqs. (3.22-3.24), we get

$$\{[\delta_{1k}\{a_0(1+\tau p+\tau_1 p^2)+p\}+\delta_{2k}](\frac{\partial^2}{\partial z^2}-\alpha^2)-[\delta_{1k}\,p+\delta_{2k}(1+\tau_0 p)]p\}\bar{T}^* = a_2[\delta_{1k}p+\delta_{2k}(1+\tau_0 p)]p(\frac{\partial^2}{\partial z^2}-\alpha^2)\bar{\phi}^* \tag{3.27}$$

$$(\frac{\partial^2}{\partial z^2}-\alpha^2-p^2)\bar{\phi}^* = a_1\bar{T}^* \tag{3.28}$$

$$(\frac{\partial^2}{\partial z^2}-\alpha^2-\frac{1}{\mu_1}p^2)\bar{\psi}^* = 0 \tag{3.29}$$

where the over-headed bar notation and super-scripted * notation are used to denote the Laplace and Hankel transform of a function respectively. p and α are representing the Laplace and Hankel transform parameters, respectively.

Now, removing $\bar{T}^*$ from (3.27) and (3.28), we get the equation having $\bar{\phi}^*$ in the following form:

$$(\frac{\partial^2}{\partial z^2}-m_1^2)(\frac{\partial^2}{\partial z^2}-m_2^2)\bar{\phi}^* = 0 \tag{3.30}$$

In the above equation, $\pm m_1$ and $\pm m_2$ are the roots of the following equation:

$$A(p)m^4 - \{2A(p)\alpha^2 + A(p)p^2 + (1+\varepsilon)B(p)\}m^2 + \alpha^2(\alpha^2+p^2)A(p) + \{(1+\varepsilon)\alpha^2 + p^2\}B(p) = 0 \quad (3.31)$$

where,

$$A(p) = \delta_{1k}\{a_0(1+\tau p + \tau_1 p^2) + p\} + \delta_{2k}$$

$$B(p) = [\delta_{1k}p + \delta_{2k}(1+\tau_0 p)]p$$

$$\varepsilon = a_1 a_2 = \frac{\gamma^2 T_0}{\rho^2 c_v c_1^2}$$

Here, ε represents the thermoelastic coupling constant.

Since the problem is taken to be symmetric, T and u are even function of z while w is an odd function of z. Thus from Eqs. (3.19-3.20), we obtain that ϕ and ψ are the even and odd functions of z, respectively. The expressions for $\bar{\phi}^*$, $\bar{\psi}^*$ and $\bar{T}^*$ are therefore given by the following forms:

$$\bar{\phi}^* = \sum_{i=1}^{2} A_i \, cosh(m_i z) \quad (3.32)$$

$$\bar{\psi}^* = C \, sinh(qz) \quad (3.33)$$

$$a_1 \bar{T}^* = \sum_{i=1}^{2} (m_i^2 - \alpha^2 - p^2) \, A_i \, cosh(m_i z) \quad (3.34)$$

where, $q^2 = \alpha^2 + \frac{1}{\mu_1} p^2$

In Eqs. $(3.32 - 3.34)$, $A_{1,}A_2$ and C are arbitrary constants which depend on both p and α but they are independent of z.

With the help of Eqs. (3.14-3.15), (3.19-3.20) and (3.32-3.34), we obtain the stresses $\bar{\sigma}_{zz}^*$ and $\bar{\sigma}_{rz}^*$ in

the following forms:

$$\bar{\sigma}_{zz}^{*} = (\frac{1}{\mu_1}p^2 + 2\alpha^2)\bar{\phi^*} + 2\alpha^2\frac{\partial\bar{\psi}^*}{\partial z} \tag{3.35}$$

$$\bar{\sigma}_{rz}^{*} = \hbar(\frac{\partial}{\partial r}(2\frac{\partial\bar{\phi}}{\partial z} + (2\frac{\partial^2}{\partial z^2} - \frac{p^2}{\mu_1})\bar{\psi})) \tag{3.36}$$

The boundary conditions (3.25) and (3.26) along with Eqs. (3.32-3.36) imply

$$\sum_{i=1}^{2}(\frac{1}{\mu_1}p^2 + 2\alpha^2)A\ cosh(m_i l) = -2\alpha^2 qC\,cosh(ql) \tag{3.37}$$

$$\sum_{i=1}^{2} m_i A\,sinh(m_i l) = \frac{1}{2}(\frac{p^2}{\mu_1} - 2q^2)C\,sinh(ql) \tag{3.38}$$

$$\sum_{i=1}^{2}(m_i^2 - \alpha^2 - p^2)A_i\,cosh(m_i l) = \frac{aa_1C_0}{\alpha p}J_1(\alpha a) \tag{3.39}$$

Therefore, the constants $A_{1,}$ A_2 and C are found from Eqs. (3.37-3.39) in the following forms:

$A_1 = -\frac{a_1(4\alpha^2 q m_2\mu_1^2 tanh(m_2 l) - (2\alpha^2\mu_1 + p^2)^2 tanh(ql))}{pX\,cosh(m_1 l)(2\alpha^2\mu_1 + p^2)^2 tanh(ql)}\theta_0^*(\alpha)$,

$A_2 = \frac{a_1(4\alpha^2 q m_1\mu_1^2 tanh(m_1 l) - (2\alpha^2\mu_1 + p^2)^2 tanh(ql))}{pX\,cosh(m_2 l)(2\alpha^2\mu_1 + p^2)^2 tanh(ql)}\theta_0^*(\alpha)$,

$C = \frac{2a_1\mu_1(m_2 tanh(m_2 l) - m_1 tanh(m_1 l))}{pX(2\alpha^2\mu_1 + p^2)\,sinh(ql)}\theta_0^*(\alpha)$,

where, $\theta_0^*(\alpha) = \frac{aC_0}{\alpha}J_{1}(\alpha a)$ and

$X = m_1^2 - m_2^2 + \frac{4\alpha^2 q\mu_1^2}{(2\alpha^2\mu_1 + p^2)^2 tanh(ql)}[m_1(m_2^2 - \alpha^2 - p^2)tanh(m_1 l) - m_2(m_1^2 - \alpha^2 - p^2)tanh(m_2 l)]$

This completes the solution in the transform domain.

3.5.2 Inversion of the Hankel Transform

Now, we define the inverse Hankel transform in the following manner

$$f^{'}(r) = \hbar^{-1}[f^*(\alpha)] = \int_0^{\infty} f^*(\alpha)\alpha J_0(\alpha r)\,d\alpha \tag{3.40}$$

Applying the inverse Hankel transform to Eqs. (3.32-3.34), we get

$$a_1 \bar{T}(r, z, p) = \int_0^\infty \alpha J_0(\alpha r) \sum_{i=1}^{2} A_i (m_i^2 - \alpha^2 - p^2) \cosh(m_i z)\, d\alpha \tag{3.41}$$

$$\bar{\phi}(r, z, p) = \int_0^\infty \alpha J_0(\alpha r) \sum_{i=1}^{2} A_i \cosh(m_i z)\, d\alpha \tag{3.42}$$

$$\bar{\psi}(r, z, p) = \int_0^\infty \alpha J_0(\alpha r)\, C \sinh(qz)\, d\alpha \tag{3.43}$$

Further, by using Eqs. (3.41-3.43) into the Eqs. (3.17-3.20), we obtain the solutions for the displacement components in the Laplace transform domain as

$$\bar{u}(r, z, p) = -\int_0^\infty \alpha^2 J_1(\alpha r) [\sum_{i=0}^{2} A_i \cosh(m_i z) + C q \cosh(qz)]\, d\alpha \tag{3.44}$$

$$\bar{w}(r, z, p) = \int_0^\infty \alpha J_0(\alpha r) [\sum_{i=1}^{2} m_i A_i \sinh(m_i z) + C \alpha^2 \sinh(qz)]\, d\alpha \tag{3.45}$$

Now, taking the Laplace transform to both sides of Eqs. (3.12-3.14) and with the help of the solutions given by Eqs. (3.41-3.45), the stress components are obtained in the Laplace transform domain as

$$\begin{aligned} \bar{\sigma}_{rr} = \textstyle\int_0^\infty \sum_{i=1}^{2} \{ \frac{2\alpha^2}{r} J_1(\alpha r) + \alpha J_0(\alpha r) (\frac{p^2}{\mu_1} - 2m_i^2) \} A_i \cosh(m_i z)\, d\alpha \\ + \textstyle\int_0^\infty 2\alpha^3 [\frac{1}{\alpha r} J_1(\alpha r) - J_0(\alpha r)] C q \cosh(qz)\, d\alpha \end{aligned} \tag{3.46}$$

$$\begin{aligned} \bar{\sigma}_{\theta\theta} = \textstyle\int_0^\infty \sum_{i=1}^{2} [\alpha J_0(\alpha r) (\frac{p^2}{\mu_1} + 2\alpha^2 - 2m_i^2) - \frac{2}{r} \alpha^2 J_1(\alpha r)] A_i \cosh(m_i z)\, d\alpha \\ - \tfrac{2}{r} \textstyle\int_0^\infty C q\, \alpha^2 J_1(\alpha r) \cosh(qz)\, d\alpha \end{aligned} \tag{3.47}$$

$$\begin{aligned} \bar{\sigma}_{zz} = \textstyle\int_0^\infty \alpha J_0(\alpha r) \{ (\frac{p^2}{\mu_1} + 2\alpha^2) [\sum_{i=1}^{2} A_i \cosh(m_i z)] \\ + 2\alpha^2 q C \cosh(qz) \}\, d\alpha \end{aligned} \tag{3.48}$$

Equations (3.41-3.48) constitute the complete set of solutions for the field variables in the Laplace transform domain.

3.5.3 Inversion of Laplace transform

3.5.3.1 Short time approximated solutions and discussions

We observe that the solutions given by Eqs. (3.41-3.48) in the previous section involve complicated functions of the Laplace transform parameter, p. Consequently, the derivation of inversion of Laplace transform analytically is a tough and formidable task. Therefore, we firstly make an attempt to get the solution for the field variables in the time domain for small values of time, and find out the locations where the function fields have discontinuities. For this purpose, we apply Boley's theorem (1962) given in Appendix-A1. We must mention that this theorem is quite advantageous (particularly, when the transform expressions involve exponential functions) in extracting the time-domain information, to find out the wave fronts and the exact values of speeds directly from the Laplace transform expressions without actually inverting these expressions.

To apply this theorem, we proceed as follows: firstly, assuming p to be very large, we expand all the quantities involving p in Eq. (3.31) in powers of $\frac{1}{p}$ and we obtain the roots of Eq. (3.31) by neglecting higher powers for smallness. Solutions for LS-model are reported in Sherief and Hamza (1994). Hence, we omit this case and concentrate on other three models we considered for our study. We obtain the roots of Eq. (3.31) for three considered models as follows:

New model-I:

$$m_1 = p(M_{11} + M_{12}\frac{1}{p} + M_{13}\frac{1}{p^2} + M_{14}\frac{1}{p^3}) \tag{3.49}$$

$$m_2 = (N_{12} + N_{12}\frac{1}{p} + N_{13}\frac{1}{p^2}) \tag{3.50}$$

New model-II:

$$m_1 = p(M'_{11} + M'_{12}\frac{1}{p} + M'_{13}\frac{1}{p^2}) \tag{3.51}$$

$$m_2 = \sqrt{p}(N'_{11} + N'_{12}\frac{1}{p} + N'_{13}\frac{1}{p^2}) \tag{3.52}$$

GN-III model:

$$m_1 = p(1 + \frac{\varepsilon}{2}\frac{1}{p} + e_{12}\frac{1}{p^2}) \tag{3.53}$$

$$m_2 = \sqrt{p}(1 + \frac{d_{22}}{2}\frac{1}{p}) \tag{3.54}$$

where,

$M_{11} = 1$, $M_{12} = 0$, $M_{13} = (\alpha^2 + \frac{\varepsilon}{a_0\tau_1})\frac{1}{2}$, $M_{14} = \{\frac{3}{8}(\frac{a_0\tau+1}{a_0\tau_1})^3 - \frac{\varepsilon}{2}(\frac{a_0\tau+1}{a_0^2\tau_1^2})\}$, $N_{11} = \sqrt{N_1}$,

$N_{12} = \frac{N_2}{2\sqrt{N_1}}$, $N_{13} = (\frac{N_3}{2} - \frac{N_2^2}{8N_1})\frac{1}{\sqrt{N_1}})$, $N_1 = \frac{c_{11}}{a_{11}}$, $N_2 = (2c_{12} - \frac{a_{12}^3}{2a_{11}^2} - 2c_{11}\frac{a_{12}}{a_{11}})\frac{1}{2a_{11}}$,

$N_3 = \{c_{11} - \frac{a_{12}^2}{a_{11}^2} + \frac{5}{8}\frac{a_{12}^4}{a_{11}^3} + \frac{1}{8b_{11}^3}(16a_{11}^2c_{11}^2 + 8b_{12}^2b_{11}b_{13} - 16a_{11}c_{11}b_{11}b_{13}) + 2c_{13} - \frac{b_{12}b_{14}}{b_{11}}\}\frac{1}{2a_{11}}$,

$a_{11} = a_0\tau_1$, $a_{12} = a_0\tau + 1$, $b_{11} = a_{11}$, $b_{12} = a_{12}$, $b_{13} = (2a_{11}\alpha^2 + a_0 + \varepsilon + 1)$,

$b_{14} = 2\alpha^2 a_{12}$, $b_{15} = 2\alpha^2 a_0$, $c_{11} = (\alpha^2 a_{11} + 1)$, $c_{12} = \alpha^2 a_{12}$,

$c_{13} = (\varepsilon_1\alpha^2 + a_{11}\alpha^4 + a_0\alpha^2)$, $c_{14} = a_{12}\alpha^4$, $c_{15} = a_0\alpha^4$,

$M'_{11} = 1$, $M'_{12} = \frac{\varepsilon}{2a'_{11}}$, $M'_{13} = \frac{\varepsilon}{2a'_{11}}(1 + \frac{1}{4a'_{11}})$,

$N'_{11} = \sqrt{N'_1}$, $N'_{12} = \frac{1}{2}\frac{N'_2}{\sqrt{N'_1}}$, $N'_{13} = \frac{N'_3}{2\sqrt{N'_1}} - \frac{N'^2_2}{8N'^{\frac{3}{2}}_1}$

$N'_1 = \frac{1}{a'_{11}}$, $N'_2 = \frac{B'_{12}}{2a'_{11}} - \frac{a_0}{a'^2_{11}}$, $N'_3 = \frac{a_0^2}{a'^3_{11}} - \frac{a_0B'_{12}}{2a'^2_{11}} + \frac{B'_{13}}{2a'_{11}}$

$B'_{12} = \frac{2}{b'_{11}}(a'_{11}c'_{11} + a_0) + \frac{2}{b'_{11}}(1 - b'_{12})$,

$B'_{13} = \frac{2}{b'_{11}}(a'_{11}c'_{11} + a_0c'_{11}) + \frac{1}{4b'^3_{11}}\{2b'_{11}b'^3_{12} - 8b'_{11}b'_{12}(a'_{11}c'_{11} + a_0)...$

$-4a'_{11}(b'^2_{12} + 2b'_{11}b'_{13})16a'_{11}(a_{11}c_{11} + a_0)\}$

$a'_{11} = a_0\tau_1$, $a'_{12} = (a_0\tau + 1)$, $b'_{11} = a'_{11}$, $b'_{12} = a'_{12}$,,

$b'_{13} = (2a'_{11}\alpha^2 + a_0 + \varepsilon_1)$, $b'_{14} = 2\alpha^2 a'_{12}$, $b'_{15} = 2\alpha^2 a_0$,

$c'_{11} = (\alpha^2 a'_{11} + 1),\ c'_{12} = \alpha^2 a'_{12},\ c'_{13} = (\varepsilon_1 \alpha^2 + a'_{11}\alpha^4 + a_0\alpha^2),$

$c'_{14} = \alpha^4 a_{12},\ c'_{15} = \alpha^4 a_0, d_{12} = \alpha^2 + \varepsilon - a_0\varepsilon,\ d_{22} = \alpha^2 - \varepsilon - a_0,\ e_{12} = \frac{4d_{12} - \varepsilon^2}{8}$

Further, for large p,

$tanh(m_i l) = tanh(ql) = 1 + O(\frac{1}{p}),\ cosh(m_i l) = \frac{1}{2}e^{m_i l} + O(\frac{1}{p}),\ sinh(ql) = \frac{1}{2}e^{ql} + O(\frac{1}{p})$

Now, substituting above values of m_1 and m_2 from (3.49-3.54) into Eq. (3.41), we get the expressions for short-time approximated solution for the temperature distribution in the Laplace transform domain for different models as follows:

New model-I:

$$\begin{aligned}\bar{T}(r,z,p) = [&\frac{(2M_{13} - \alpha^2)}{p^3}\int_0^\infty \alpha J_0(\alpha r)\,\theta_0^*(\alpha)\,e^{m_1(z-l)}d\alpha + \frac{(2M_{13} - \alpha^2)}{p^3} \\ &+ \frac{(2M_{13} - \alpha^2)}{p^3}\int_0^\infty \alpha J_0(\alpha r)\,\theta_0^*(\alpha)\,e^{-m_1(z+l)}d\alpha] + O(\frac{1}{p^4}) \\ &+ [\frac{1}{p}\int_0^\infty \alpha J_0(\alpha r)\,\theta_0^*(\alpha)\,e^{m_2(z-l)}d\alpha \\ &+ \frac{1}{p}\int_0^\infty \alpha J_0(\alpha r)\,\theta_0^*(\alpha)\,e^{-m_2(z+l)}d\alpha] + O(\frac{1}{p^2})\end{aligned} \tag{3.55}$$

New model-II:

$$\begin{aligned}\bar{T}(r,z,p) = [&\frac{M'_{12}}{p^2}\int_0^\infty \alpha J_0(\alpha r)\,\theta_0^*(\alpha)\,e^{m_1(z-l)}d\alpha + \\ &+ \frac{M'_{12}}{p^2}\int_0^\infty \alpha J_0(\alpha r)\,\theta_0^*(\alpha)\,e^{-m_1(z+l)}d\alpha] + O(\frac{1}{p^3}) \\ &+ [\frac{1}{p}\int_0^\infty \alpha J_0(\alpha r)\,\theta_0^*(\alpha)\,e^{m_2(z-l)}d\alpha \\ &+ \frac{1}{p}\int_0^\infty \alpha J_0(\alpha r)\,\theta_0^*(\alpha)\,e^{-m_2(z+l)}d\alpha] + O(\frac{1}{p^2})\end{aligned} \tag{3.56}$$

GN-III model:

$$\bar{T}(r,z,p) = [\frac{\varepsilon}{p^2}\int \alpha J_0(\alpha r)\,\theta_0^*(\alpha)\,e^{m_1(z-l)}d\alpha$$
$$+\frac{\varepsilon}{p^2}\int_0^\infty \alpha J_0(\alpha r)\,\theta_0^*(\alpha)\,e^{-m_1(z+l)}d\alpha] + O(\frac{1}{p^3})$$
$$+[\frac{1}{p}\int_0^\infty \alpha J_0(\alpha r)\,\theta_0^*(\alpha)\,e^{m_2(z-l)}d\alpha$$
$$+\frac{1}{p}\int_0^\infty \alpha J_0(\alpha r)\,\theta_0^*(\alpha)\,e^{-m_2(z+l)}d\alpha] + O(\frac{1}{p^2}) \tag{3.57}$$

Now, we apply Boely's theorem (see Appendix-A1) as follows:

The inverse Laplace transform of the first term in Eq. (3.55) is

$$I_1 = \frac{1}{2\pi i}\int_{d-i\infty}^{d+i\infty}\frac{(2M_{13}-\alpha^2)}{p^3}\int_0^\infty \alpha J_0(\alpha r)\,\theta_0^*(\alpha)\,e^{m_1(z-l)+pt}d\alpha\,dp$$

which can be written as

$$I_1 = \frac{1}{2\pi i}\int_{d-i\infty}^{d+i\infty}\frac{K'}{p^3}[1+O(\frac{1}{p})]\,e^{g(p,t)}dp \tag{3.58}$$

where, $K' = (2M_{13}-\alpha^2)\,e\int_0^\infty \alpha J_0(\alpha r)\,\theta_0^*(\alpha)\,e^{m_1(z-l)+pt}d\alpha$, and $g(p,t) = m_1(z-l)+pt$.

By using Eq. (3.49), we obtain $g(p,t) - p\xi(t) = O(\frac{1}{p})$, where, $\xi(t) = M_{11}(z-l)+t$.

Similarly, we can invert the remaining terms in Eq. (3.55).

The inverse Laplace transform of the first term in Eq. (3.56) is

$$I_2 = \frac{1}{2\pi i}\int_{d-i\infty}^{d+i\infty}\frac{M'_{12}}{p^2}\int_0^\infty \alpha J_0(\alpha r)\,\theta_0^*(\alpha)\,e^{m_1(z-l)+pt}d\alpha\,dp$$

which can be written as

$$I_2 = \frac{1}{2\pi i}\int_{d-i\infty}^{d+i\infty}\frac{K'}{p^2}[1+O(\frac{1}{p})]\,e^{g(p,t)}dp \tag{3.59}$$

where, $K' = M'_{12}e^{-M'_{12}(z-l)}\int_0^\infty \alpha J_0(\alpha r)\,\theta_0^*(\alpha)\,e^{m_1(z-l)+pt}d\alpha$, and $g(p,t) = m_1(z-l)+pt$.

By using Eq. (3.51), we obtain $g(p,t) - p\xi(t) = O(\frac{1}{p})$, where, $\xi(t) = M'_{11}(z-l)+t$.

Similarly, we can invert the remaining terms in Eq. (3.56).

The Inverse Laplace transform of the first term in Eq. (3.57) is

$$I_3 = \frac{1}{2\pi i}\int_{d-i\infty}^{d+i\infty} \frac{\varepsilon}{p^2}\int_0^{\infty} \alpha J_0(\alpha r)\,\theta_0^*(\alpha)\,e^{m_1(z-l)+pt}d\alpha\,dp$$

which can be written as

$$I_3 = \frac{1}{2\pi i}\int_{d-i\infty}^{d+i\infty} \frac{K'}{p^2}[1+O(\frac{1}{p})]\,e^{g(p,t)}dp \tag{3.60}$$

where, $K' = \varepsilon\int_0^{\infty} \alpha J_0(\alpha r)\,\theta_0^*(\alpha)\,e^{m_1(z-l)+pt}d\alpha$, and $g(p,t) = m_1(z-l)+pt$.

By using Eq. (3.53), we obtain $g(p,t) - p\xi(t) = O(\frac{1}{p})$, where, $\xi(t) = (z-l)+t$.

Similarly, we can invert the remaining terms in Eq. (3.57).

3.5.4 Discussion on analytical results

In this section, we will analyze the results obtained as short-time approximated solutions in the previous section. Inverting all four terms in Eqs. (3.55) and (3.56) in the form as given in Eqs. (3.58) and (3.59), we note that in cases of new model-I and new model-II, the first and second terms of the solution given for temperature field represent the waves originating at the upper surface of the plate $(z = l)$ and the lower surface of the plate $(z = -l)$, respectively. The expressions for M_{11} and M'_{11} indicate that the waves propagate with the finite speed unity in the contexts of these two models. These waves are modified elastic waves and arrive at the middle plane at time l. The third and fourth terms in Eqs. (3.55) and (3.56) are clearly not of wave type, but diffusive, which is due to the presence of the damping term in the new heat conduction equation. Similarly, under GN-III model, the first and the second terms in Eq. (3.57) represent the modified elastic waves originating at the upper and lower surface of the plate and the elastic wave propagate with the same non dimensional finite speed 1. Moreover, like the cases of new models, the third and fourth terms in this case are diffusive in nature. From equations (3.49-3.50) and (3.53), it follows that the speed of modified elastic wave is 1 under all three models: new model-I, new model-II and GN-III model. The solution as given in Eqs. (3.49) and (3.51) further predicts that elastic waves under new model-I

propagate without any attenuation while in the case of new model-II, the elastic wave propagates with attenuation and the attenuation coefficient is M'_{12} which depends on the thermoelastic coupling constant as well as on delay parameter τ. The elastic wave for GN-III model also decays exponentially with the attenuating coefficient $\varepsilon/2$. Therefore, we can conclude that although the speed of modified elastic wave does not depend on delay term τ and the new heat conduction models is similar in nature with GN-III model, but the elastic wave decays exponentially with different attenuating coefficients pertinent to new model-I, new model-II and GN-III model. Further, the new model-I shows no attenuation in elastic wave. This indicates distinct feature of the present new model-I.

By following Boley's theorem (1962) as given above, we note that the solution as derived for different models reveal an interesting fact: the temperature function has no discontinuity in the contexts of new model-I and new model-II. This is also similar in nature like GN-III model which also predicts no such discontinuity for temperature distribution.

We have also found that the solution of stress components consist of six different parts. Four parts represent four coupled waves: two (modified elastic and shear waves) originating at the upper surfaces, and two (modified elastic and shear waves) originating at the lower surface of the plate. Other two parts are diffusive in nature. For new model-I and II, each and every stress components surfers a finite jump discontinuity at the wave fronts $\xi(t) = (z-l)+t$. However, the stress components are continuous across the shear wave front $\frac{1}{\sqrt{\mu_1}}(z-l)+t=0$. Further, the shear waves propagate with the common non dimensional finite speed $\sqrt{\mu_1}$. The displacement u and its first partial derivative with respect to z and t are also continuous functions, but its second derivatives are discontinuous functions with a finite jump. The displacement w is also continuous. The thermal parts of all the field variables are diffusive in cases of new model-I, new model- II as well as in the case of GN-III model. Our results for GN-III model match with the corresponding results for GN-III model as reported by Mukhopadhyay and Kumar (2010). By comparing our results with the corresponding results in the context of LS-model (see Sherief and Hamza (1994)), a significant difference is observed. In the context of LS-model as reported in Sherief and Hamza(1994), the

solution of temperature distribution in the middle plane of the plate consists of four coupled waves: two modified elastic waves originating from the upper and lower surfaces of the plate and two thermal waves propagating from the upper and lower surfaces of the plate. Both the modified elastic wave as well as modified thermal wave propagate with finite speeds. Furthermore, all these wave attenuate with an exponential decay. Similarly, other fields also consists of modified thermal wave propagating with finite speed and with constant attenuating coefficients. It must also be mentioned that in the contexts of dual phase-lag and three phase-lag models, the thermal wave propagate with finite speed as reported by Mukhopadhyay and Kumar (2010). Hence, we find here a significantly different nature of the solutions predicted by the present model that takes into account a single delay term as compared to the results predicted by LS-model that includes one thermal relaxation parameter or by the other generalized thermoelastic models like, dual phase-lag and three phase-lag models. However, the new model-II shows closely related predictions like GN-III model.

3.6 Numerical examples

In the previous section, we have made an attempt to investigate the nature of solutions of the field variables by deriving the short-time approximated analytical solutions with the help of Boley's theorem (1962). Now, in order to understand the differences of behavior of field variables in the present contexts, we carry out numerical work to compute the numerical values of physical fields at the middle plane of the plate at any instant of time. We consider the copper material for the purpose of numerical work and assume the following data as given in Chandrasekharaiah and Srinath(1997): $\lambda = 7.76\times 10^{10}\mathrm{Nm}^{-2}$, $\mu = 3.38\times 10^{10}\mathrm{Nm}^{-2}$, $\alpha_t = 1.78\times 10^{-5}\mathrm{K}^{-1}$, $d = \frac{K}{\rho c_e} = 0.000113\mathrm{m}^2\mathrm{s}^{-1}$, $c_e = 383.1\mathrm{JKKg}^{-1}$, $\rho = 8954\mathrm{Kgm}^{-3}$, $T_0 = 293\mathrm{K}$, $\eta = \frac{1}{d}$, $\tau = 0.1$, $\tau_1 = \frac{\tau^2}{2}$, $C_0 = 1$, $l = 1$, $K^* = \frac{c_v(\lambda+2\mu)}{4}$

We have employed the numerical method given by Bellman *et al.* (1966) (see Appendix-A2) to invert the Laplace transforms. We apply the Gauss-Laguerre integration method to invert the Hankel transforms. By using programming in MatLab, we carry out our computation to obtain the

numerical values of physical fields in the physical domain (r, t) by using the solutions obtained in Laplace transform domain given by Eqs. (3.41-3.48). The non-dimensional finite speed of the elastic wave is computed to be 1 for new model-I and II. The elastic wave reaches the middle plane at non-dimensional time 1 for both the new model-I and new model-II. This is also found to be the same for GN-III model.

The physical fields are computed at the middle plane of the plate for different values of r and t from Eqs. (3.41-3.48). For the purpose of comparing the results in the contexts of new models with the corresponding results under LS-model, we also carry out our computation for LS model by assuming $\tau_0 = 0.2$. We represent the numerical results graphically and show the variations of different fields at three non-dimensional times $(0.35, 0.69, 1.21)$. Figures $(3.1, 3.3, 3.5)$ show the distributions of temperature, displacement and radial stress, respectively in the contexts of all four models for the delay parameter $\tau = 0.1$ and for thermal relaxation parameter of LS model, $\tau_0 = 0.2$. Figures $(3.2, 3.4, 3.6)$ are displayed separately to compare the distributions of the variables under only three models: new model-I, new model-II, and GN-III model to understand the difference in prediction for field variables by these models. The curves at times $(0.35, 0.69)$ in Figures $(3.1 - 3.6)$ are showing the distributions of the fields in the middle plane before the arrival of the elastic wave. The curves at time 1.21 in Figures $(3.1 - 3.6)$ are showing the distributions of the fields after the arrival of the elastic wave to the middle plane of the plate under different models.

It follows from Figures $(3.1, 3.2)$ that under all models, the temperature decreases with the increase of time and region of influence increases with time. Furthermore, before the arrival of elastic wave to the middle plane, this field shows different values under different models near the boundary and the difference decreases with the increase of radial distance. However, at later time after the arrival of elastic wave to the middle plane, there is no significant differences among the results predicted by three models: new model-I, new model-II and GN-III model. We note that the results predicted by LS-model shows a prominent difference as compared to the results predicted by other three models. This difference is more prominent before the arrival of elastic wave to the middle plane. The nature of distribution of displacement fields can be observed from Figures $(3.3, 3.4)$ which

show that there is a significant change in the distribution after the elastic wave reaches the middle plane of the plate and the region of influence increases significantly. However, all models agrees with a similar trend of distribution. Difference of results is noted for LS-model and other three models, although at initial time this difference is not very prominent. With the increase of radial distance and time, this difference becomes very prominent. Variation of radial stress is depicted in Figures $(3.5, 3.6)$ which show that for this field also, there is a prominent difference in the nature of radial stress distribution before and after the arrival of elastic wave to the middle plane of the plate. Before the arrival of elastic wave, the radial stress is compressive up to a longer region of the middle plane, but it becomes tensile in nature after the arrival of elastic wave in the middle plane. However, there is no prominent increment in the region of influence with the increment of time. Further more, we observe that GN-III model, new model-I and new model-II indicate similar results for this field variable too. However, LS-model indicate a significantly different values as compared to the other three models. This difference is more prominent at initial time of interaction. At time 1.21, i.e., after the arrival of the elastic wave at the middle plane, the difference decreases. The displacement component w vanishes at the middle plane of the plate and difference among different models for the other stress components are found to be similar to those for the radial stress components. Hence, we have omitted these figures. Figures $(3.7 - 3.9)$ are plotted to show the variation of the physical fields under all four models by assuming the delay parameter $\tau = 0.01$ and thermal relaxation parameter of LS-model $\tau_0 = 0.02$ and we observe that the differences in prediction under different models reduces with the smaller values of delay parameter and thermal relaxation parameters. Figures $(3.10 - 3.12)$ show the variations of the physical fields under all four models, at time $t = 0.02$, i.e. at very small time. We note that at smaller time, the disagreement of LS model with other three models is very much significant for all the field variables. Moreover, at small time, the results under GN-III model closely match with the corresponding results under new model-II.

The variation of the physical fields with time at two different locations of the middle plane of the plate are displayed separately in Figures $3.13(a, b)$, $3.14(a, b)$ and $3.15(a, b)$ in which $3.13(a)$,

$3.14(a)$ and $3.15(a)$ show the variation of the field variables with time at $r = 0.5$, i.e near the boundary while $3.13(b)$, $3.14(b)$ and $3.15(b)$ show the variation of field variables with time at $r = 2.5$, i.e at the mid position of the middle plane of the plate. We observe that there is more prominent disagreement of LS model as compared to other models for the prediction of temperature distribution at the the mid position as compared to the position near the boundary. Figure $3.14(a, b)$ reveal that there is no significant differences in the variation of displacement with time near the boundary as well as at the mid position of the middle plane under different models. However, the prediction of radial stress distribution by LS model near the boundary as well as at the mid position of the middle plane of the plate is significantly different as compared to the predictions by other three models.

3.7 Conclusions

We make an attempt to investigate the specific features of the heat conduction model that is very recently proposed by Quintanilla (2011). This model is an alternative reformulation of three phase-lag model to overcome the fact that the three phase-lag model defines ill-posed problem. We consider a problem of thick plate subjected to axi-symmetric temperature distribution at the lower and upper surface.

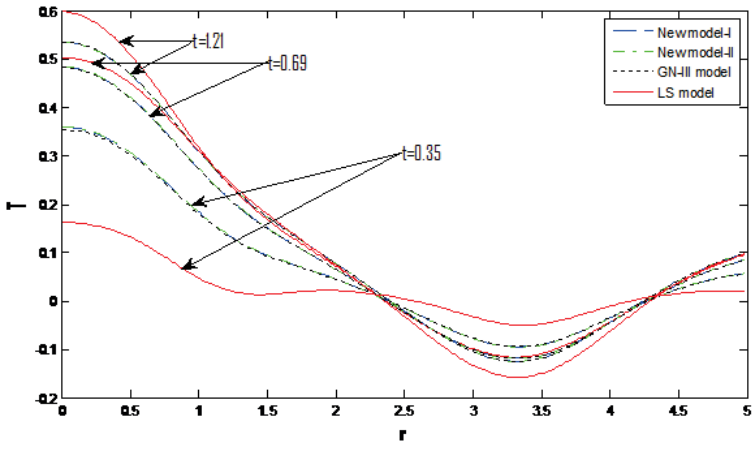

Fig. 3.1 Temperature distribution in the middle plane of the plate with $\tau = 0.1$ and $\tau_0 = 0.2$

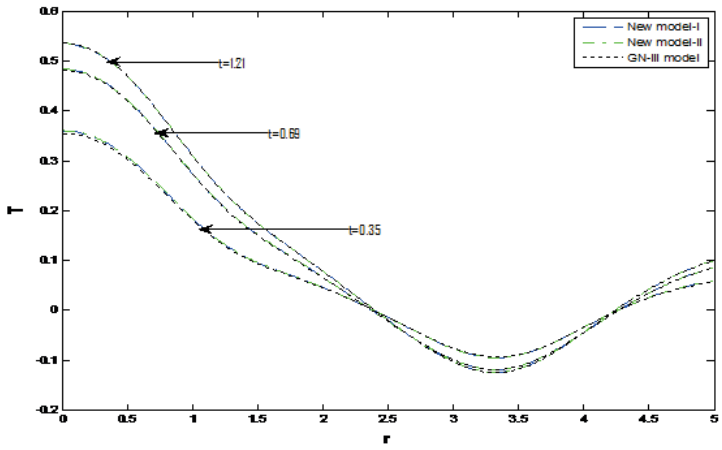

Fig. 3.2 Temperature distribution in the middle plane of the plate with $\tau = 0.1$ and $\tau_0 = 0.2$

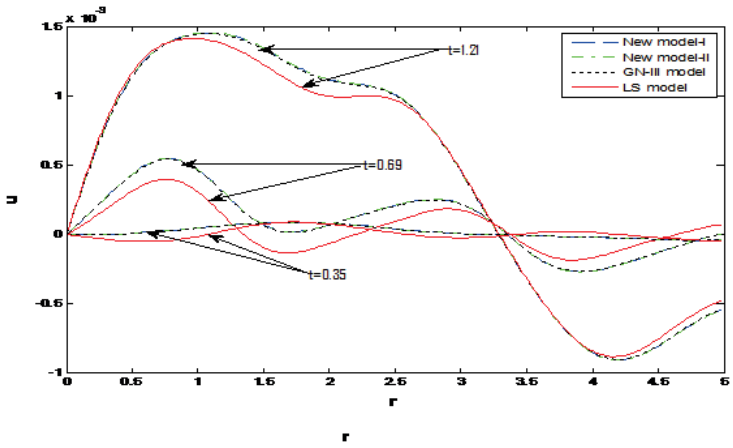

Fig. 3.3 Displacement distribution in the middle plane of the plate with $\tau = 0.1$ and $\tau_0 = 0.2$

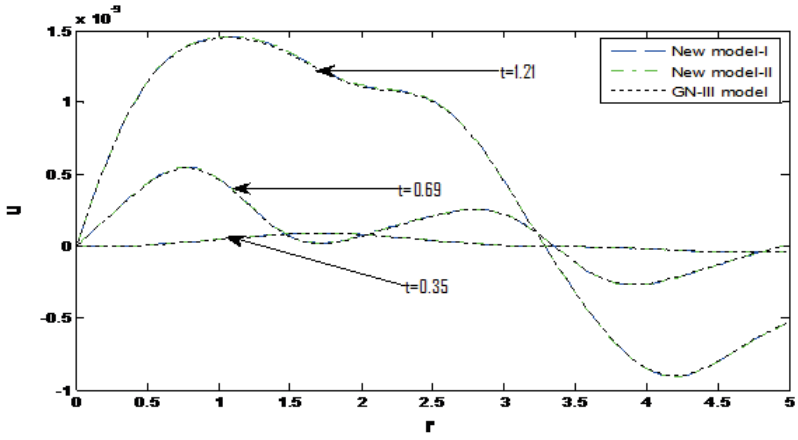

Fig. 3.4 Displacement distribution in the middle plane of the plate with $\tau = 0.1$ and $\tau_0 = 0.2$

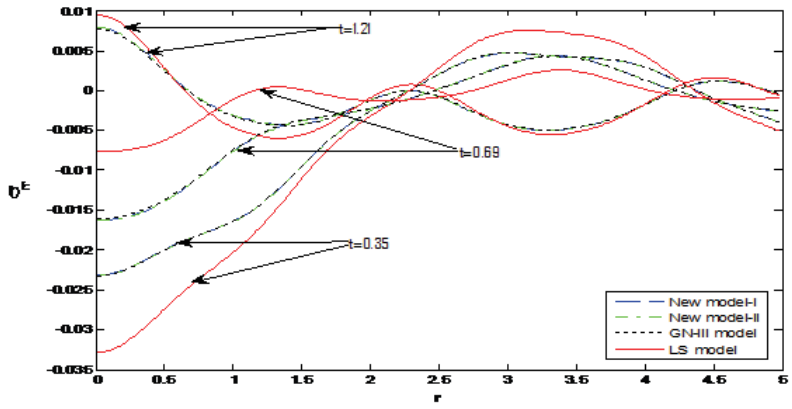

Fig. 3.5 Radial Stress distribution in the middle plane of the plate with $\tau = 0.1$ and $\tau_0 = 0.2$

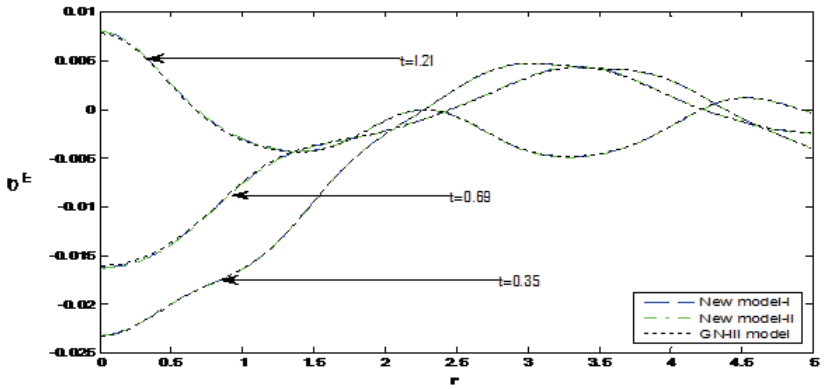

Fig. 3.6 Radial Stress distribution in the middle plane of the plate with $\tau = 0.1$ and $\tau_0 = 0.2$

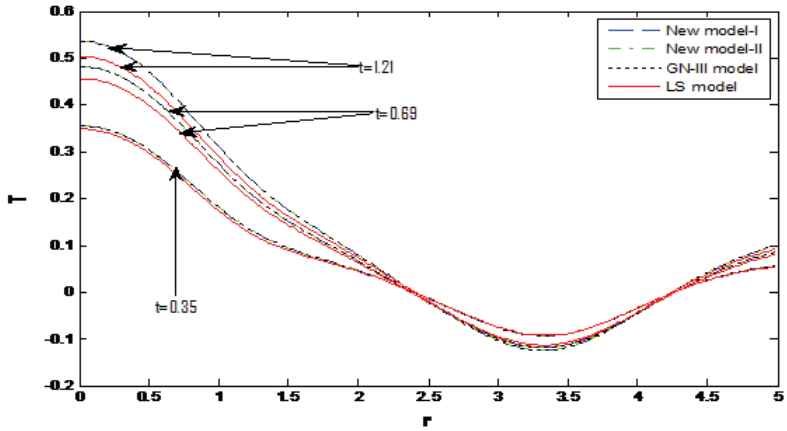

Fig. 3.7 Temperature distribution in the middle plane of the plate with $\tau = 0.01$ and $\tau_0 = 0.02$

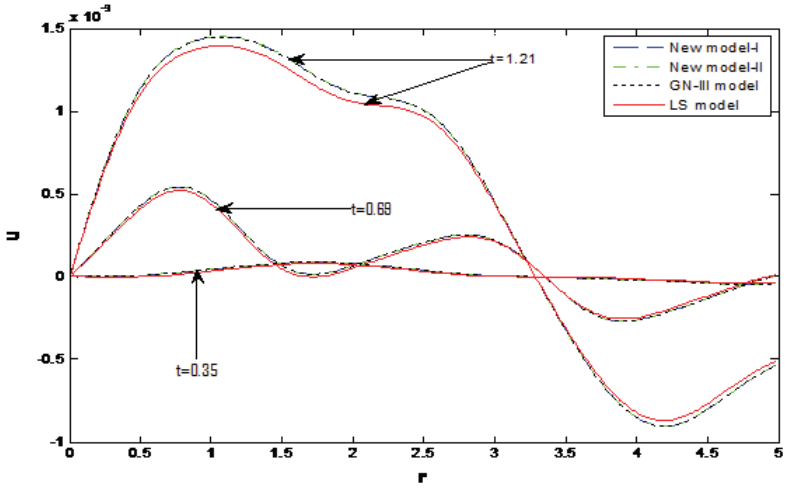

Fig. 3.8 Displacement distribution in the middle plane of the plate with $\tau = 0.01$ and $\tau_0 = 0.02$

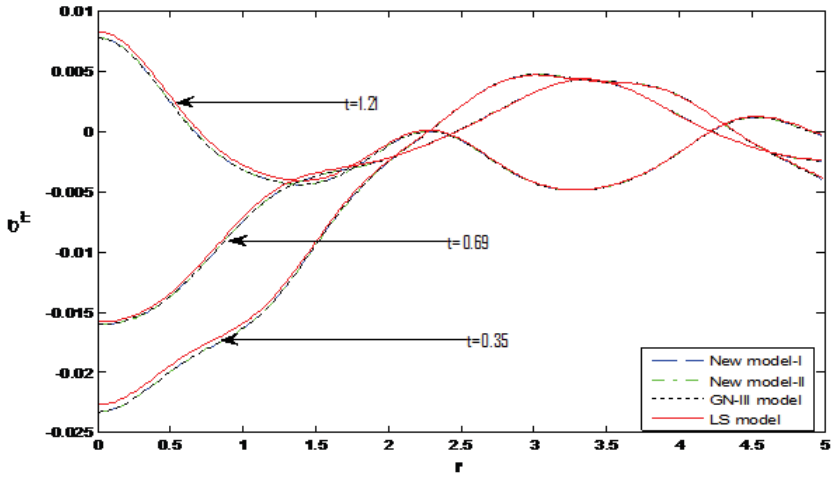

Fig. 3.9 Stress distribution in the middle plane of the plate with $\tau = 0.01$ and $\tau_0 = 0.02$

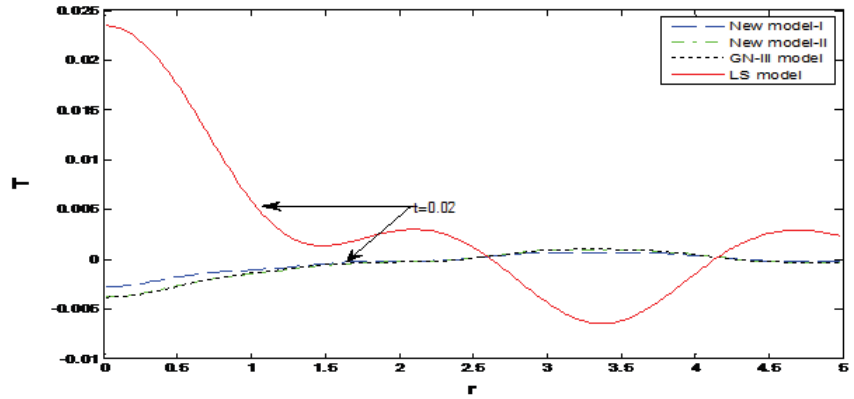

Fig. 3.10 Temperature distribution in the middle plane of the plate with $\tau = 0.1$ and $\tau_0 = 0.2$

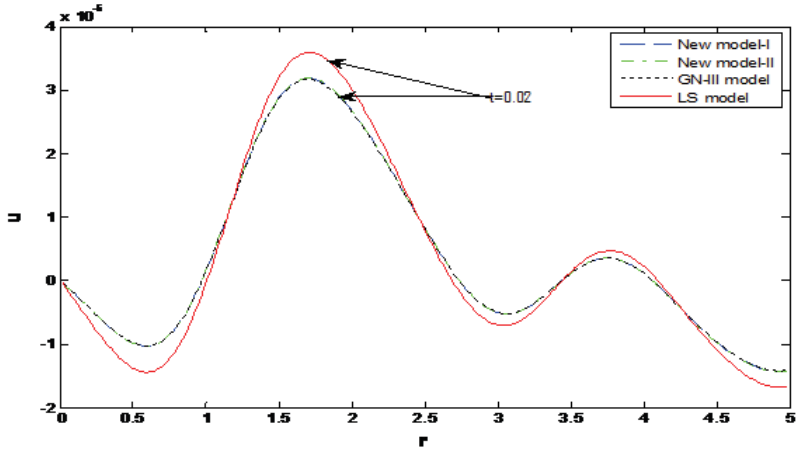

Fig. 3.11 Displacement distribution in the middle plane of the plate with $\tau = 0.1$ and $\tau_0 = 0.2$

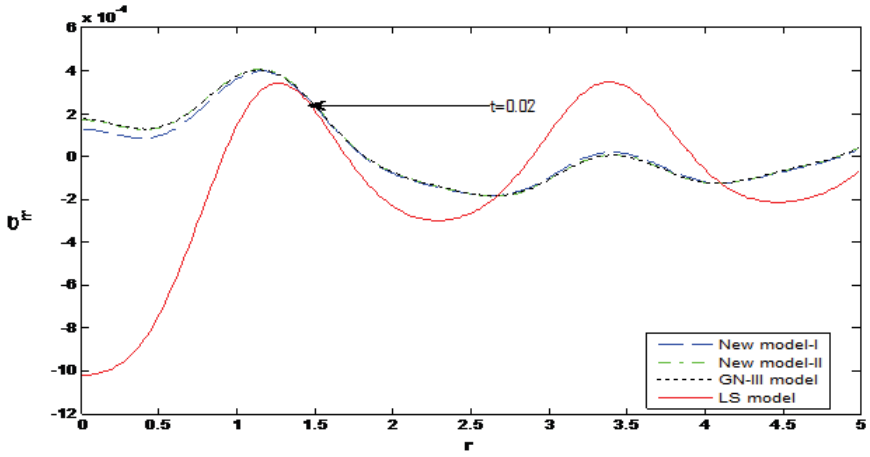

Fig. 3.12 Stress distribution in the middle plane of the plate with $\tau = 0.1$ and $\tau_0 = 0.2$

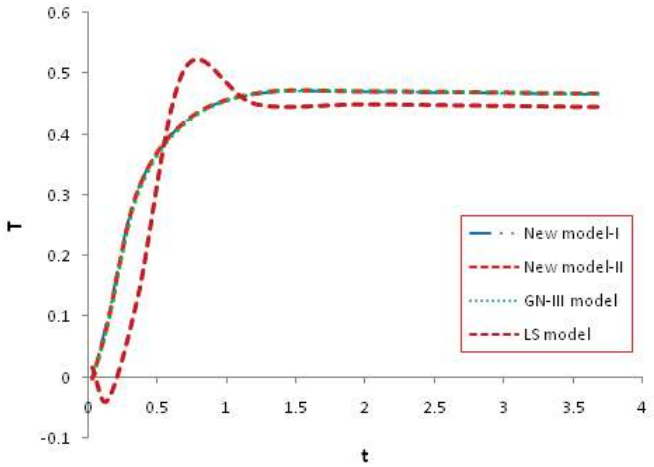

Fig. 3.13 (a) Variation of Temperature with time at *r=0.5* for $\tau = 0.1$ and $\tau_0 = 0.2$

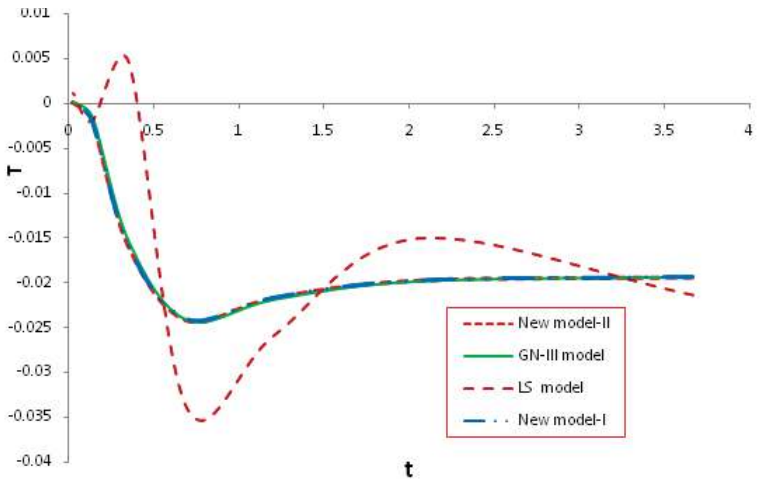

Fig. 3.13 (b) Variation of Temperature with time at *r=2.5* for $\tau = 0.1$ and $\tau_0 = 0.2$

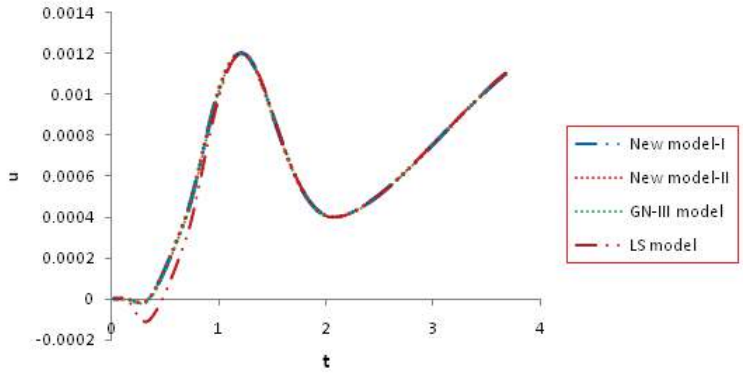

Fig. 3.14 (a) Variation of displacement with time at *r=0.5* for $\tau = 0.1$ and $\tau_0 = 0.2$

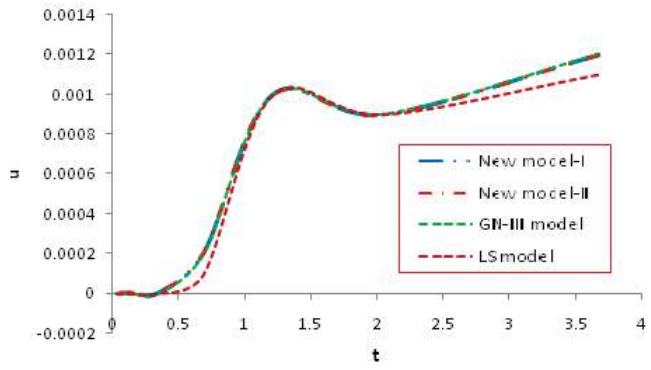

Fig. 3.14 (b) Variation of displacement with time at *r=2.5* for $\tau = 0.1$ and $\tau_0 = 0.2$

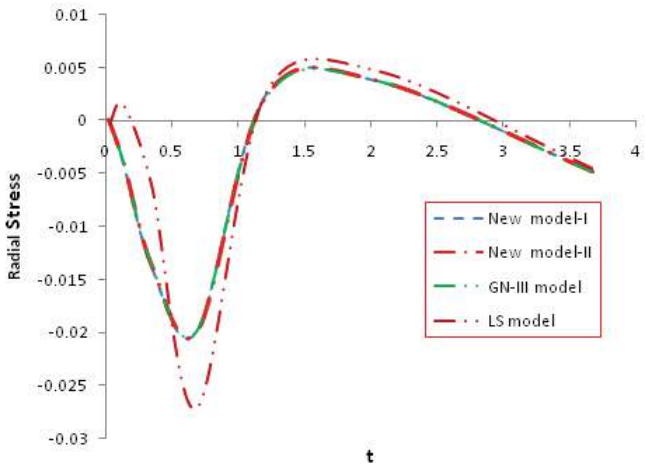

Fig. 3.15 (a) Variation of Radial stress with time at *r=0.5* for $\tau = 0.1$ and $\tau_0 = 0.2$

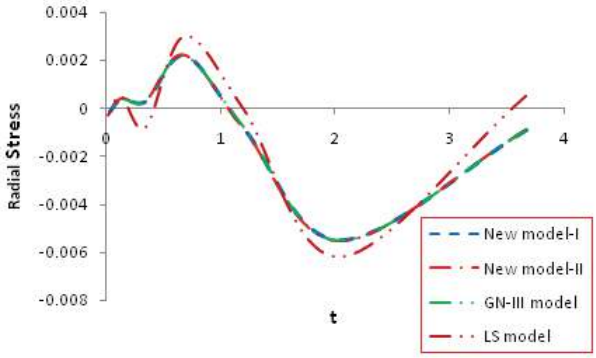

Fig. 3.15 (b) Variation of Radial stress with time at *r=2.5* for $\tau = 0.1$ and $\tau_0 = 0.2$

- Under all models, the temperature decreases with increase of time and region of influence increases with time. Furthermore, before the arrival of elastic wave to the middle plane, this field shows different values under different models near the boundary and the difference decreases with the increase of radial distance.

- For distribution of displacement field, there is a significant change in the distribution after the elastic wave reaches the middle plane of the plate and the region of influence increases very significantly. However, all models agrees with a similar trend of distribution. Difference of results is noted for LS-model and other three models, although at initial time this difference is not very prominent.

- There is a prominent difference in the nature of variation of stress fields before and after the arrival of elastic wave to the middle plane of the plate. Before the arrival of elastic wave, the radial stress is compressive up to a longer region of the middle plane.
- Lord-Shulman model shows prominently different results as compared to other three models for all the physical field variables.
- New model-I and new model-II show similar predictions like GN-III model for all the physical field variables.